Chinese Chemical Letters 36 (2025) 110234

Contents lists available at ScienceDirect

Chinese Chemical Letters

journal homepage: www.elsevier.com/locate/cclet

The advanced development of innovative photocatalytic coupling strategies for hydrogen production

Yuehai Zhi[a,1], Chen Gu[a,1], Huachao Ji[a], Kang Chen[a], Wenqi Gao[b], Jianmei Chen[a,*], Dafeng Yan[b,*]

[a] College of Electronic and Optical Engineering & College of Flexible Electronics (Future Technology), Nanjing 210023, China
[b] Hubei Key Laboratory for Precision Synthesis of Small Molecule Pharmaceuticals & Ministry of Education Key Laboratory for the Synthesis and Application of Organic Functional Molecules & College of Chemistry and Chemical Engineering, Hubei University, Wuhan 430062, China

ARTICLE INFO

Article history:
Received 21 May 2024
Revised 5 July 2024
Accepted 10 July 2024
Available online 10 July 2024

Keywords:
Photocatalysis
Pollutants removal
Valorization of organics
Catalyst design

ABSTRACT

Photocatalytic technology harnesses solar energy to facilitate chemical transformations, presenting significant potential in energy generation and environmental remediation. However, the conventional O_2 evolution process is hindered by high reaction barriers and inefficiencies, which limit its widespread application. Therefore, exploring novel photocatalytic coupling strategies to replace water oxidation has become a key route to enhance the efficiency of H_2 production. In this review, organic pollutants removal and the valorization of organics as substitutes for water oxidation coupling strategies for photocatalytic H_2 production are comprehensively summarized. These strategies not only circumvent the high reaction barriers associated with O_2 evolution to enhance the H_2 production but also aid in the removing of organic pollutants or synthesis of value-added chemicals. We also present future research directions and underscore the significance of advanced catalyst design, in-depth analysis of reaction mechanisms, and systematic optimization strategies in realizing an efficient and sustainable photocatalytic process. This guidance is anticipated to provide theoretical and practical new insights for the future development of photocatalytic coupling reactions, fostering further explorations in the realm of renewable energy and environmental governance.

1. Introduction

The current global energy landscape is at a transformative juncture, predominantly driven by the urgent need to reduce reliance on fossil fuels and to mitigate the adverse effects of widespread pollutant generation [1–4]. Photocatalytic generation of clean H_2 emerges as a promising solution that marries the development and utilization of renewable resources with profound environmental remediation [5–10]. Photocatalysis, a process driven by solar irradiation, employs photoactive materials to initiate and sustain chemical reactions conducive to H_2 generation and is one of the cleanest forms of energy transformation. However, due to the high energy barrier associated with the oxidation of water, the overall efficiency of photocatalytic water splitting is limited. Thus, to enhance photocatalytic efficiency and broaden its practical application, it is imperative to develop novel approaches to supplant the traditional water oxidation process [11–14].

A highly prospective method is to couple with the photocatalytic oxidation of pollutants, which not only removes recalcitrant organic contaminants to prevent environmental pollution but also enables, in certain cases, the synthesis of valuable products for industrial chemical production, effectuating a waste-to-wealth transformation [15]. Sun *et al.* have engineered Z-scheme heterostructure photocatalysts with staggered band structures that synergize organic pollutant degradation with concurrent oxidation reactions and H_2 formation reaction, significantly boosting H_2 production efficiency [16–19]. Furthermore, by designing specific catalysts, it is possible to convert pesticide and pharmaceutical residues into nontoxic compounds and, in some instances, generate commercially valuable intermediates, extending the applications beyond mere energy production. In the realm of green chemistry, the application of photocatalytic technology is also of paramount importance. Through photocatalytic reactions, organic pollutants and hazardous chemicals can be efficiently degraded, transforming them into harmless byproducts, thus purifying the environment

* Corresponding authors.
E-mail addresses: chenjianmei@njupt.edu.cn (J. Chen), dafengyan@hubu.edu.cn (D. Yan).
[1] These authors contributed equally to this work.

https://doi.org/10.1016/j.cclet.2024.110234
1001-8417/

and safeguarding the health of ecosystems. By the coupling strategies, the well-known technology of photocatalytic water splitting can concomitantly degrade organic and inorganic pollutants and even pathogens. The key to this complex coupling process is to optimize the photodegradation process to maximize H_2 output while ensuring the complete mineralization of contaminants, rendering them harmless. This transformative approach holds the potential to convert waste streams into a source of energy in the form of H_2, delivering dual ecological benefits [20–22]. On the other hand, coupling photocatalytic H_2 production with the valorization of organic molecules effectively circumvents the high reaction barriers associated with O_2 generation. Photocatalytic water splitting involves the absorption of photons by semiconductor materials, generating electron-hole pairs that drive the redox reactions to produce H_2 and O_2. The oxygen evolution reaction (OER) is a significant challenge due to its high overpotential, which limits the overall efficiency. To overcome this, the development of efficient co-catalysts such as transition metal oxides can lower the OER energy barrier. Additionally, optimizing the photocatalyst structure through the construction of heterojunctions and nanocomposites can enhance charge separation and reduce recombination. Stability issues can be addressed by surface passivation and doping with stable elements, which prevent photocorrosion and maintain high catalytic activity. In the coupled process of photocatalytic H_2 production and organic valorization, photonic energy can be utilized to reduce water molecules to H_2 while transforming $^{\bullet}OH$ radicals or other organic precursors into value-added chemicals, such as benzimidazoles and furfural [23,24]. This coupled reaction not only reduces the dependence on O_2 evolution but also enhances the overall conversion rate of solar energy. The design and reaction tuning of such photocatalysts not only increase the efficiency of H_2 production but also yield chemicals with practical industrial applications. It is much necessary to summarize the advanced development of innovative photocatalytic coupling strategies for H_2 production [25,26].

In this review, we initially provide a brief overview of the current state of traditional photocatalytic water splitting. Subsequently, our focus primarily lies in the exploration of photocatalytic oxidation of pollutants and the valorization of organic molecules. Concrete examples of these alternative oxidative reactions coupled with H_2 production are presented [27]. Unlike most other commentaries, we do not extensively dwell on the classification and design of the catalysts themselves. Instead, we underscore the significance of the strategies of these two coupled systems, which are crucial for the future design and efficiency enhancement of photocatalysts. It is anticipated that the guidance offered by this article will provide new theoretical and practical perspectives for the future development of photocatalytic coupled reactions, promoting further exploration in the fields of renewable energy and environmental remediation.

2. General description of innovative photocatalytic coupling strategies for H_2 production

The process of photocatalytic water splitting, under the influence of photon irradiation, divides water molecules into H_2 and O_2. This reaction typically involves the use of semiconductor materials as photocatalysts, with TiO_2 being one of the most prevalent [28]. Photocatalysts are capable of absorbing photons to generate electron-hole pairs. And these electrons and holes migrate along the conduction and valence bands of the catalyst, respectively, promoting the progression of the water-splitting reaction. While promising as a sustainable energy solution, photocatalytic water splitting efficiently converts solar energy into clean H_2 fuel [29]. However, there remain inherent limitations to its widespread application. The OER in traditional photocatalytic water splitting encounters a high energy barrier, which imposes constraints on its broad applicability [30]. Moreover, the produced electrons and holes are prone to recombine within the semiconductor material [31], rather than participating in the water-splitting reaction, which further reduces the photocatalytic efficiency [32]. To address these challenges, researchers are dedicating efforts to the development of novel photocatalytic materials and the optimization of catalyst structures to enhance the separation efficiency of charge carriers. Additionally, effective oxidative alternative reactions are being sought out to significantly improve H_2 production efficiency (Fig. 1). In applications encompassing contaminant abatement to the symbiotic formation of organic compounds [33], photocatalysis not only facilitates the breakdown of deleterious compounds, thus purifying the environment [34], but also transmutes these compounds into valuable feedstocks or energy sources such as H_2 or other organic molecules, demonstrating efficiency in energy utilization and environmental compatibility [35]. Given that photocatalysis chiefly operates on renewable sources like solar light, devoid of external electricity demands, the mechanism heralds considerable potential in championing sustainable development and fostering the principles of green chemistry [36].

This review explores an innovative photocatalytic water splitting method using catalysts to speed up the reaction. When exposed to light, electrons in the catalyst are excited from the valence band to the conduction band, creating electron-hole pairs [37]. These electrons are captured in the conduction band to generate H_2 at the cathode while avoiding recombination with holes. Meanwhile, the anode engages holes to drive side reactions for the synthesis of high value chemicals instead of merely evolving O_2, a process that, while environmentally beneficial, offers limited commercial and energetic returns [38]. O_2 as a byproduct holds modest economic gain, and its evolution commonly incurs considerable overpotential, diminishing the overall energy efficiency of the reaction. In contrast, the production of commercially valuable

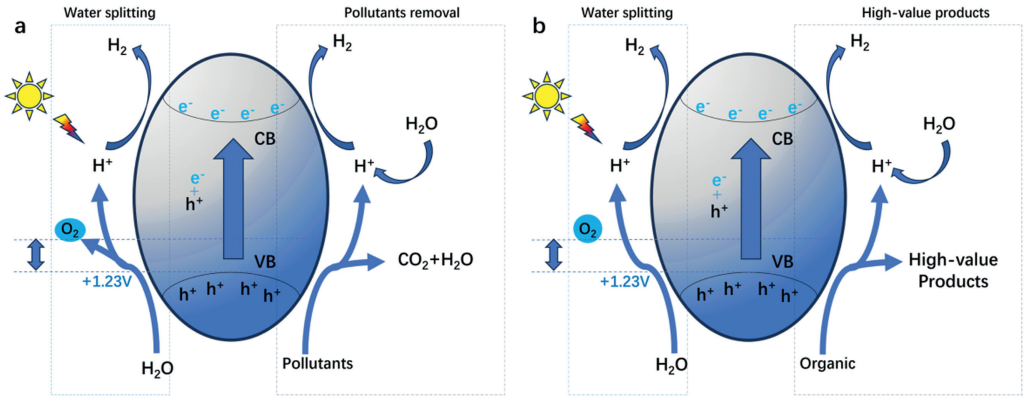

Fig. 1. Innovative mechanism of photocatalysis: (a) The coupling of pollutants removal and H_2 production; (b) The coupling of valorization of organic and H_2 production.

chemicals at anode presents a significant advantage [39]. These high value products can financially bolster the water-splitting process, enhancing its commercial appeal [40]. Furthermore, eschewing O_2 generation can reduce the requisite overpotential under certain conditions, thus enhancing energy efficiency. The demand for such products could foster the commercialization of this technology, providing a viable and marketable method for storing renewable energy sources [41], such as solar energy. Moreover, tailoring the photocatalytic process to co-generate H_2 and valuable organic compounds not only increases catalyst utilization efficiency but also broadens the scope of photocatalysis applications [42]. An in-depth exploration of the impact of high value product generation on the energy input and output efficiency is necessary, as is the assessment of photocatalyst performance and the influence of this strategy on reaction selectivity [43]. When exploring novel photocatalytic materials, employing first-principles computational methods to comprehend the material's electronic structure and band characteristics is imperative. For instance, by modulating the material's band structure and introducing defects or doping, the absorption capability of visible light can be enhanced, facilitating efficient charge carrier separation. Integrating theoretical designs with experimental approaches enables the development of novel materials exhibiting superior photocatalytic performance. In terms of material synthesis, advanced synthesis techniques such as *in-situ* synthesis, templating, and hydrothermal methods offer promising avenues [44]. For instance, employing *in-situ* synthesis methods allows for the introduction of dopants or functional groups during the material's growth process, enabling precise control over the material's structure and morphology. Additionally, utilizing templating methods facilitates the fabrication of materials with specific morphologies and pore structures, thereby enhancing photocatalytic performance. Regarding performance characterization, employing various characterization techniques for comprehensive analysis is essential. For instance, utilizing transmission electron microscopy (TEM) and scanning electron microscopy (SEM) enables the observation of material morphology and structure. Techniques like X-ray photoelectron spectroscopy (XPS) and Fourier-transform infrared spectroscopy (FTIR) offer insights into the surface chemical composition and structural characteristics of materials. Overall, this review underscores the importance of optimizing application efficiency and creating economic value through specially designed photocatalytic systems, offering new research directions and expanding the horizon for the practical deployment and commercial viability of photocatalytic water splitting technology [45].

3. Pollutants removal coupling with H_2 production

Photocatalytic reactions have vast potential for addressing pollutants removal and H_2 production through water splitting [46]. For various types of pollutants, photocatalytic reactions can achieve efficient oxidative removal, utilizing the generated electron-hole pairs to facilitate water splitting for H_2 production. Recent research indicates significant progress in implementing photocatalytic technology for simultaneous pollutant degradation and H_2 production through water splitting.

In the case of organic pollutants such as benzene [47], formaldehyde [48], and heavy metal ions [49], photocatalytic technology can effectively degrade these pollutants by generating highly reactive hydroxyl radicals ($^{\bullet}OH$) and other intermediate species [50]. Additionally, photocatalysis can utilize the generated electron-hole pairs to split water molecules and produce H_2, offering an environmentally friendly and efficient approach to clean energy production. Recent studies demonstrate that specific structural designs and surface modifications of photocatalysts can achieve efficient degradation of various organic pollutants, while also improving the photocatalytic water splitting efficiency. This represents a significant exploration of the synergistic application of water splitting for H_2 production and pollutants removal. Advancements in the development of efficient photocatalytic systems for wastewater purification and the transformation of solar energy into clean H_2 fuel have been substantial [51]. In the realm of environmental remediation and organic compound transformation, specific cases highlight the tangible impacts of photocatalytic technology. For instance, in pollutant removal applications, photocatalysis has been effectively employed to degrade organic dyes and pharmaceutical residues in industrial wastewater. In a study, researchers utilized a photocatalytic reactor to treat wastewater containing organic dyes [52]. Through photocatalytic degradation, the organic dyes were efficiently removed, achieving compliance with environmental standards and thereby facilitating effective wastewater treatment. This review concentrates on innovative strategies to enhance the performance of photocatalysts and to increase the rate of electron transfer to address the rapid recombination of photogenerated charge carriers.

Zhang *et al*. has unveiled an innovative photocatalytic nanocomposite, composed of MoS_2 quantum dots, anchored on $ZnIn_2S_4$ and reduced graphene oxide (RGO) substrate (5% MoS_2 QDs@$ZnIn_2S_4$@RGO1) [53]. This material has demonstrated remarkable photocatalytic prowess, particularly in the abatement of natural organic matter from industrial dye effluent [54]. Under illumination, $ZnIn_2S_4$ activates electron excitation, which is transferred to the MoS_2 quantum dots and RGO layered, thereby driving H_2 production effectively. Dye molecules secured to the catalyst surface similarly undergo excitation, prompting electron migration to the conduction bands of $ZnIn_2S_4$ or RGO. These electrons are then harnessed by MoS_2 quantum dots, further catalyzing H_2 generation (Fig. 2a). Remarkably, hydrogen evolution is also spurred by electrons originating directly from $ZnIn_2S_4$ and organic matter oxidized by photogenerated holes, independent of dye-sensitized processes. Comprehensive assessments of this catalytic capability to degrade an array of organic dyes and pollutants, including rhodamine B (RhB) [55], eosin Y (EY) [56], fulvic acid (FA), methylene blue (MB), and *p*-nitrophenol (PNP) [57], revealed exceptional degradation efficiencies of MB and EY at 98.5% and 98.6%, correspondingly, with concurrent TOC removal rates of 80% and 84% (Fig. 2b). Furthermore, the composite exhibited a pronounced hydrogen evolution during RhB degradation, achieving a significant 45.33 mmol over 12 h. However, hydrogen was not detected during MB degradation (Fig. 2c). This nanocomposite enhances photocatalytic performance by optimizing the electron transfer pathways and dynamics [58]. This investigation offers an efficacious stratagem for enhanced water treatment and photocatalytic H_2 generation, employing well-engineered nanocomposites for potent pollutant degradation and energy conversion [59]. This breakthrough paves a new pathway for environmental remediation and the development of sustainable energy resources.

Li *et al*. made significant strides in developing enzyme-mimicking nano-catalysts for photocatalysis in a groundbreaking study [60]. They have introduced an innovative material that integrates photosensitive redox reactions with biomimetic catalysis. Through one single-step synthesis, they crafted OVs-TiO_2/Pd hybrid nanosheets enriched with OVs and precisely controlled Pd content. These nanosheets exhibit enhanced oxidation and hydrogenase-like activities, efficiently facilitating antibiotic decomposition and H_2 generation [61]. The material demonstrates a remarkable synergetic effect, elevating both the photocatalytic and enzyme-mimicking capacities, thus opening new avenues for the application of multifunctional nanostructures. Under the illumination of a 300 W incandescent lamp, the OVs-TiO_2/Pd nano-catalysts unveil their unique photocatalytic mechanism. The generation of charge carriers, stimulated by photons, is facilitated across an 'electron bridge' formed by OVs, enabling electron transfer from the

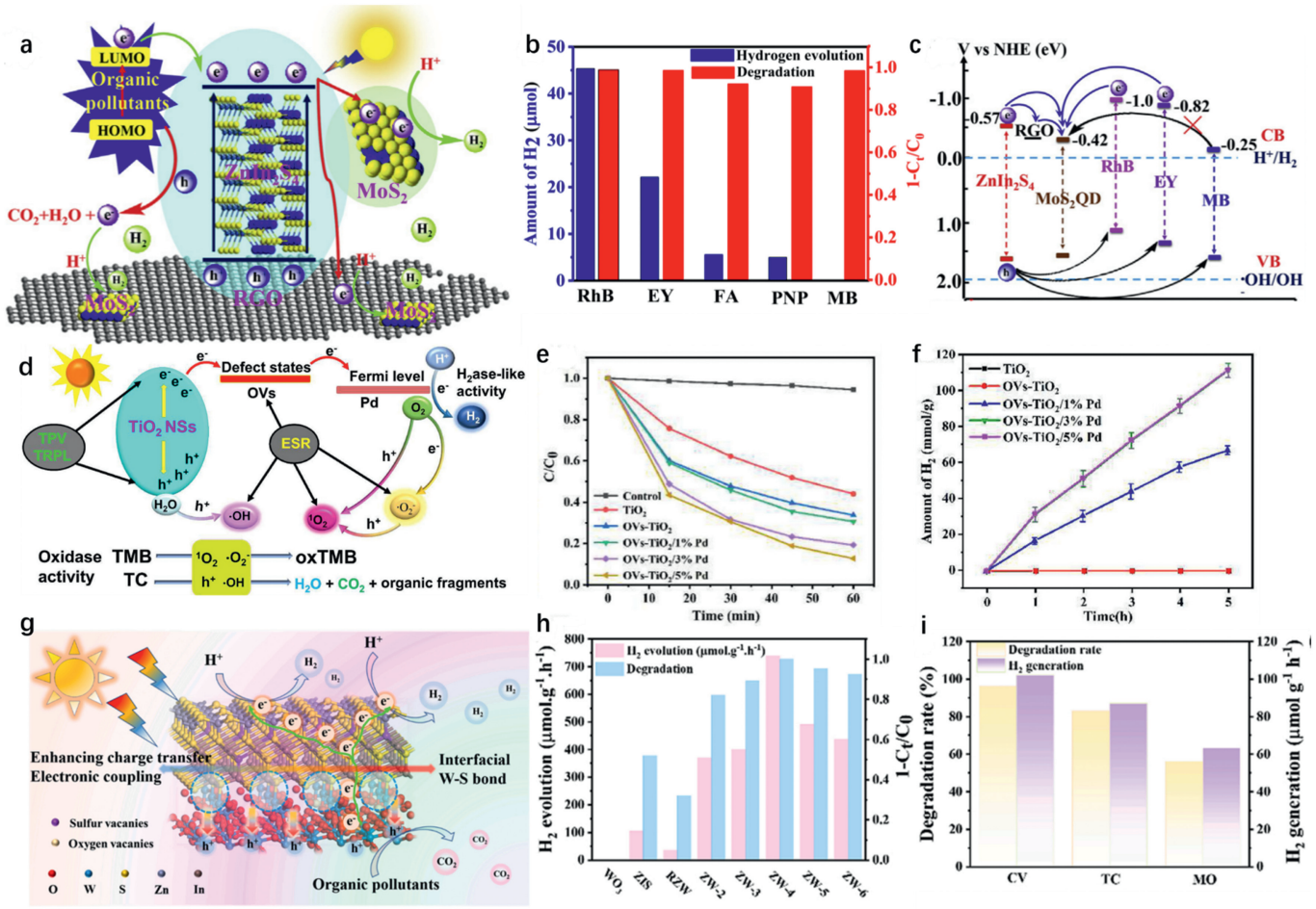

Fig. 2. (a) Illustration of pollutant degradation, electron flow and energy conversion. (b) H_2 production and simultaneous pollutant degradation over $5MoS_2$@$ZnIn_2S_4$@RGO1 under simulated solar light for 12 h. (c) Energy band illustration of different samples. Copied with permission [53]. Copyright 2017, Elsevier. (d) The possible mechanism of catalytic reaction under light irradiation condition. (e) Kinetics of photodegradation of TC over a series of samples under visible light ($\lambda > 420$ nm). (f) TiO_2, OVs-TiO_2, and OVs-TiO_2/Pd HNSs with various Pd contents: H_2 production curves. Copied with permission [60]. Copyright 2023, Elsevier. (g) Plausible mechanism for the PPH over ZW. (h) H_2 generation and RhB degradation for 4 h. (i) The degradation rate and H_2 generation of CV, TC and MO. Copied with permission [64]. Copyright 2024, Elsevier.

semiconductor to Pd NCs. This mechanism allows H^+ and O_2 adsorbed on the nano-catalyst to acquire electrons from Pd nanoparticles, resulting in the generation of H_2 and superoxide anions ($^{\bullet}O^{2-}$) [62]. These $^{\bullet}O^{2-}$ interact with adsorbed O_2 and water, leading to the production of H_2O and the formation of singlet oxygen ($^1O_2$) and $^{\bullet}OH$. Ultimately, tetracycline (TC) undergoes degradation into H_2O, CO_2, and smaller organic fragments by the nano-catalyst (Fig. 2d). The efficacy of the OVs-TiO_2/Pd nanosheets in degrading TC was thoroughly investigated, highlighting the catalytic potential at varying Pd NCs loadings for hydrogenase-like synergy. Observations show a modest increase in H_2 production rate to 0.245 mmol g^{-1} h^{-1} with the introduction of OVs (Fig. 2e). Fine-tuning the loading of Pd NCs maximizes active sites and optimizes H_2 generation. Excessive loading of Pd NCs, however, was found to potentially obscure other active sites, leading to a saturation point in catalytic activity enhancement (Fig. 2f). In summary, the outstanding photocatalytic performance of the OVs-TiO_2/Pd nanocatalysts, particularly in the realms of environmental remediation and clean energy production, holds promising prospects. The current study delves into the synergistic interplay between photocatalysis and enzyme mimicking, offering invaluable insights for the design and application of innovative nano-catalysts in the future [63].

Innovative Z-scheme heterojunctions have been spotlighted for their proficiency in photocatalytic processes [64]. Sun *et al.* introduced an ultrafine $ZnIn_2S_{4-x}$-WO_{3-x} heterostructure catalysts, which was synthesized through an *in-situ* hydrothermal route. This construction fostered interface bonding, fine-tuning the electronic architecture, expanding the internal electric field, and diminishing charge pile-up at interface vacancies. The proposed PPH mechanism for ZW-4 under visible light involves both ZIS and WO_3 contributing electrons and holes. Due to the Z-scheme, the CB electrons of WO_3 recombine with the VB holes of ZIS *via* interface bonds, while the CB electrons of ZIS migrate to surface sulfur vacancies and WO_3 absorbs holes (Fig. 2g). The photocatalytic performance was remarkably enhanced under visible-light, realizing efficient H_2 evolution and pollutant degradation (Fig. 2h). WO_3 was identified as suboptimal for H_2 generation and RhB decomposition due to its inadequate conduction band potential. Among investigated photocatalysts ZW-4 exhibited superior H_2 production (737.75 μmol g^{-1} h^{-1}) and complete RhB eradication (removal rate >99.99%) (Fig. 2i). The exceptional capabilities of ZW-4 are attributable to its unique structural intricacies and composition, which foster favorable electronic properties and catalytic efficiencies. Notably, regulated interface gaps in the heterostructure boosted charge transfer and exciton partitioning [65], key mechanisms elucidated through comparative photocatalyst analyses. Broad applicability of ZW-4 was demonstrated *via* concurrent H_2 generation and diverse contaminant degradation, employing distillery wastewater as a testbed. Such results underscore the

extensive potential of ZW-4, not just in H_2 production but also in effective degradation of complex wastewater contaminants, a promising avenue for industrial applications in waste management and clean energy. These sulfur vacancies also act as sites for H^+ reduction, thus amplifying H_2 evolution, which is integral to the hydroxylation-assisted degradation of RhB [66].

Photocatalytic technology integrates pollutant oxidation with water splitting to efficiently remove pollutants while producing clean hydrogen energy, offering a green and sustainable solution [67]. The recent research achievements provide important theoretical and practical foundations for the synergistic application of photocatalytic water splitting and pollutant removal, thereby indicating the direction for further advancements in this field.

4. Valorization of organics coupling with H_2 production

The burgeoning field of integrated energy conversion and chemical synthesis is pivotal to efficient material processing [68]. The concurrent generation of H_2 and high value chemicals through photocatalysis supports sustainable development while facilitating greener synthesis routes. In the context of photocatalytic technology, the design of active sites plays a crucial role in maneuvering the selectivity and activity of the catalyst, particularly for coupling organic synthesis with H_2 production. In the context of photocatalytic technology, the design of active sites plays a crucial role in maneuvering the selectivity and activity of the catalyst, particularly for coupling organic synthesis with H_2 production. Engineering the electronic structure through the creation of heterojunctions or composite materials can enhance charge separation and reduce recombination rates. For example, constructing type-II or Z-scheme heterojunctions can facilitate efficient electron-hole pair separation, thereby improving the overall photocatalytic activity. Additionally, introducing defects or vacancies can create localized states that act as active sites for enhanced reactivity. Advancements in this field hinge on novel heterojunctions and co-catalytic systems that underpin enhanced charge dynamics and separation, as illustrated by DFT-informed designs like Ni-doped quantum dots and TiO_2 microspheres. Furthermore, optimally decorated semiconductor frameworks, such as Pd/ZnO nanosheets, offer a radical approach for efficient photocatalytic transformations. Core-shell architectures, including $Mo_2C@ZnIn_2S_4$ and zirconium-based MOFs, also play a role in pushing the frontiers of photocatalytic efficiency. Lastly, innovative strategies for photocatalytic biomass conversion in water exemplify the successful application of this technology for sustainable chemical production. Studies indicate that photocatalytic reactions can convert biomass-derived compounds into high-value biofuels or chemicals. For example, researchers utilized photocatalytic technology to convert biomass-derived compounds into the biofuel ethanol, enabling the effective utilization of renewable resources while reducing reliance on traditional petrochemical products [69]. By presenting these specific cases, we can vividly illustrate the practical efficacy of photocatalytic technology in environmental remediation and organic compound transformation, further emphasizing its significance and potential in the field of sustainable development. Future research will continue to perfect these complex material systems, tailoring them for the increasingly demanding dual objectives of economic viability and environmental stewardship.

4.1. Converting biomass waste coupling with H_2 production

Given the increasing demand for renewable energy and green chemicals, there has been a growing focus on utilizing biomass waste as a rich and renewable resource. The efficient conversion of biomass waste [70], particularly the realization of its HER and the modification processes, has become a major research hotspot. Photocatalyst technology, with its mild reaction conditions, efficient energy utilization, and selective reactivity, has emerged as a crucial method in achieving this objective. Recent research findings have demonstrated that the application of photocatalyst technology in the HER process of biomass waste can significantly enhance reaction efficiency and H_2 production rates [71]. By designing and synthesizing highly efficient catalytic photocatalysts, researchers have successfully converted solar energy into the energy required for the reaction, facilitating the efficient hydrolysis reaction of biomass waste and further promoting H_2 generation. In comparison to traditional thermochemical methods, photocatalyst technology not only reduces energy consumption [72], but also has the potential to minimize the generation of side reactions, thereby enhancing the selectivity of H_2 production. Furthermore, photocatalyst technology has been successfully applied to the modification process of biomass waste. By matching appropriate photocatalysts and reaction conditions, researchers have achieved the selective conversion of specific compounds in biomass waste [73], obtaining high-value organic chemicals, such as acids. This process has not only increased the resource value of biomass waste but also provided a new avenue for the green and high-value utilization of biomass waste.

However, photocatalyst technology still faces several challenges in the HER and modification processes of biomass waste. These include the synthesis and optimization of photocatalysts [74], control of reaction conditions, catalyst stability, recycling usage, and further improvement of reaction efficiency. Future work will focus on the continued application of photocatalyst technology in this field, with theoretical simulations and experimental research being utilized to address current challenges, thereby aiding in the efficient conversion and sustainable utilization of biomass waste.

You *et al.* developed a h-ZnSe/Pt@TiO_2 hollow type-II heterojunction consisting of ZnSe and O_2-rich vacancy modified TiO_2 [75]. The newly designed heterojunction demonstrated excellent photocatalytic activity for the conversion of cellulose into H_2 and formic acid in water. This significant finding holds promise for the utilization of biomass resources in a sustainable and efficient manner. The enhanced photocatalytic performance of the h-ZnSe/Pt@TiO_2 catalyst for cellulosic refining, as depicted in Fig. 3a. Under illumination, ZnSe and TiO_2 undergo excitation, generating electrons and holes. The S-scheme heterojunction formed at the interface between ZnSe and TiO_2 facilitates the efficient recombination of holes and electrons, promoting effective charge separation. This synergistic effect maintains the high reducibility of ZnSe and the high oxidizability of TiO_2. Notably, the recombination of the VB holes of ZnSe with the CB of TiO_2 electrons act as a self-generated hole scavenger, effectively suppressing ZnSe photodegradation and enhancing the stability of the photocatalyst. Furthermore, the coexistence of highly reducible electrons and highly oxidizable holes provides a substantial driving force for H_2 evolution and cellulose degradation, resulting in accelerated reactions in pure water. The conversion of common biomass into H_2 through photorefining in neutral aqueous solution using the h-ZnSe/Pt@TiO_2 photocatalyst was investigated. Substrates, including ball-milled α-cellulose, wood, paper, and grass, were utilized, and the H_2 yields were determined as 14386, 11655, 12855, and 12156 μmol/g, respectively, based on the results from Fig. 3b. The photocatalytic production rates of formic acid using h-ZnSe/Pt@TiO_2 were examined for different cellulose sources. Ball-milled α-cellulose, wood, paper, and grass (200 mg each) were utilized as substrates. As depicted in Fig. 3c, formic acid yields of 372, 234, 251, and 248 μmol g^{-1} h^{-1} were obtained for α-cellulose, wood, paper, and grass [76], respectively. The sequential degradation of glucose through oxidation and formate elimination, resulting in the formation of gluconic acid, xylulose, and ribose (Fig. 3d). The initial oxidation of glucose produces gluconic acid, which in turn undergoes formate elimination

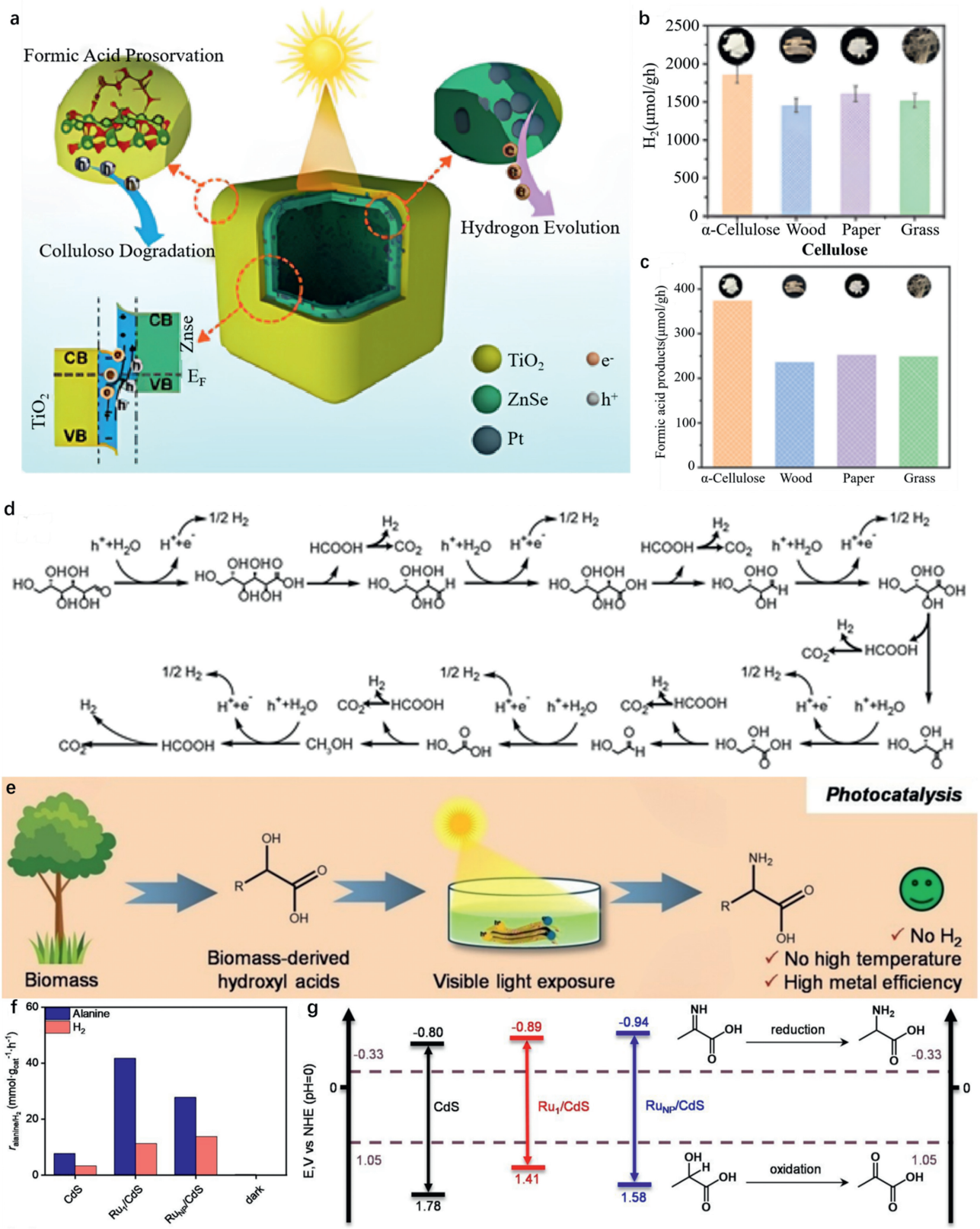

Fig. 3. (a) Schematic diagram of the proposed mechanism for the enhanced photocatalytic cellulose reforming for H_2 and formic acid of h-ZnSe/Pt@TiO_2. (b) H_2 production of h-ZnSe/Pt@TiO_2 with various cellulose sources. (c) Formic acid production of h-ZnSe/Pt @TiO_2 with various cellulose sources. (d) The proposed degradation process of glucose during photocatalytic reaction. Copied with permission [75]. Copyright 2024, Wiley-VCH. (e) The photocatalytic conversion of biomass-derived β-hydroxy acids into amino acids under light irradiation. (f) The hydrogen generation performance related to the amination process. (g) The band diagrams for CdS, Ru1/CdS, and RuNP/CdS. Copied with permission [78]. Copyright 2024, Wiley-VCH.

to yield xylulose. The presence of formate plays a crucial role during the early stages of the reforming process. Furthermore, xylulose is oxidized to generate xylonic acid [77], followed by subsequent formate elimination leading to the degradation of xylonic acid to ribose. This iterative process of formate elimination continues until the solution contains only formate.

Li *et al.* achieved remarkable visible light catalysis with the Ru1/CdS catalyst, efficiently converting biomass-derived α-hydroxy acids into amino acids [78]. Using a simple deposition/precipitation method, they successfully synthesized ruthenium single-atom catalysts on CdS nanosheets (Ru1/CdS) (Fig. 3e). Under visible light irradiation and mild conditions, this catalyst effectively converts biomass-derived β-hydroxy acids into amino acids. The introduction of ruthenium not only promotes alanine production but also enhances hydrogen generation [79]. However, the hydrogen production rate of RuNP/CdS surpasses that of Ru1/CdS, indicating that the introduction of Ru single atoms facilitates electron transfer to lactate, thereby promoting alanine production, while Ru nanoparticles promote electron transfer to H_2O, facilitating hydrogen production (Fig. 3f). To investigate the band structure of lactate amination, they utilized Mott-Schottky plots to determine the conduction band potentials of Ru1/CdS, RuNP/CdS, and CdS. Finally, they integrated all data to establish a comprehensive electron diagram satisfying the redox potential from lactate to alanine (Fig. 3g). Through the aforementioned studies, researchers have achieved selective conversion of specific compounds in biomass waste, successfully obtaining high-value organic chemicals [80]. These research findings provide important theoretical and practical guidance for the application of photocatalytic technology in energy generation and environmental protection, laying a solid foundation for future sustainable development and green chemical production.

4.2. Converting BA to BAD coupling with H_2 production

The selective oxidation of aldehyde molecules is a crucial functional group transformation in organic electro synthesis [81]. The O_2-containing derivatives produced from these reactions are typically used as important, versatile intermediates in the synthesis of pharmaceuticals and fine chemicals. During this process, the aldehyde and hydroxymethyl groups at the 2-carbon and 5-carbon positions of the furan ring can be converted into various high-value products through a variety of chemical reactions [82]. Photocatalytic technology can achieve coupled production of aldehydes and H_2 in the process of aldehyde production. This method combines the efficient properties of photocatalysis with the significant applications of aldehyde products, providing new possibilities for green chemistry. By utilizing photocatalysis to produce aldehydes coupled with H_2 [83], can not only achieve high aldehyde yields, but it also promotes the sustainable production of H_2 energy. The development of this technology presents new prospects in the field of organic synthesis and simultaneously drives the advancement of renewable energy and the production of green chemicals.

Liu *et al.*'s research presents a dual-functional redox system, CdS/U6N, which combines photocatalytic H_2 production with selective organic synthesis [84]. By combining two photocatalysts with well-matched bandgaps and band structures, and leveraging the advantages of a staggered heterojunction, the redox capabilities of both photocatalysts can be maximized, thereby improving the efficiency of photocatalytic water splitting for H_2 production.

In the CdS/U6N heterojunction, the possible mechanism for the coupled photocatalytic H_2 production and benzyl alcohol (BA) conversion to benzaldehyde (BAD) can be described as follows (Fig. 4a). Under light irradiation, the unique electron transfer pathway in the type II heterojunction leads to the interaction between photogenerated holes in U6N and benzyl alcohol. Initially, the α-C of benzyl alcohol is oxidized, generating $^{\bullet}$CH(OH)Ph. Subsequently,

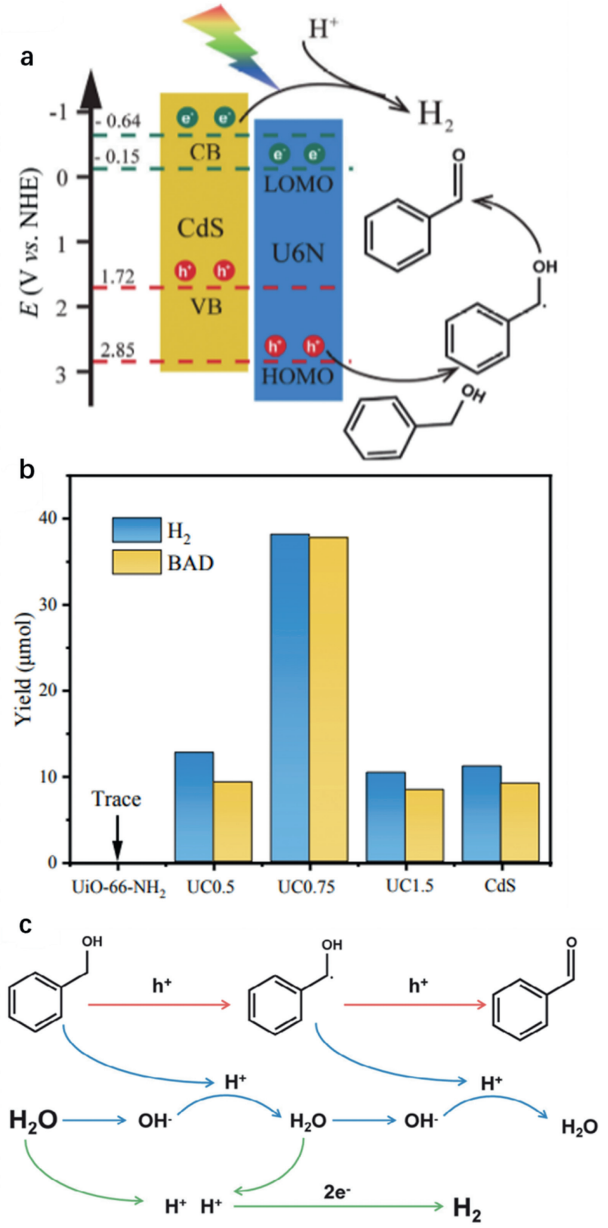

Fig. 4. (a) Proposed reaction mechanism for photoredox dual reaction for BA conversion and H_2 evolution over CdS/U6N S-scheme heterojunction under light irradiation. (b) The photocatalytic activities of H_2 evolution and BAD production on U6N, CdS, and UCx composites in 3 h. (c) Two-step single-electron oxidation and reduction mechanism of BA and H_2O. Copied with permission [84]. Copyright 2024, Wiley-VCH.

further oxidation occurs, resulting in the formation of BAD. Simultaneously, the photogenerated electrons in CdS combine with the H^+ generated during the reaction, leading to the production of H_2. Under the illumination of a 300 W xenon lamp, the photocatalytic H_2 production and oxidation of BA to form BAD were studied in an aqueous solution (Fig. 4b). CdS exhibited moderate H_2 and BAD generation rates of 11.1 μmol and 9.1 μmol [85], respectively, while U6N displayed negligible H_2 production and BA oxidation. However, after the formation of the UCx heterojunction, the photocatalytic performance significantly improved. Among them, the UC0.5 composite provided H_2 and BAD products of 12.7 μmol and 9.3 μmol, respectively. When the loading amount of CdS was further increased, the UC0.75 composite exhibited the best photocatalytic performance, with H_2 and BAD production reaching

38.1 μmol and 37.8 μmol, approximately three times higher than that of pure CdS [86]. However, as the loading amount continued to increase, the photocatalytic performance of the UC1.5 composite decreased. This can be attributed to the light shielding effect caused by the accumulation of CdS nanoparticles. Researching the two-step single-electron oxidation-reduction [87] mechanism of BA and H_2O provides insights into the source of H_2 in the coupled photocatalytic HER and BA oxidation (Fig. 4c). The oxidation reaction of BA is controlled by H^+ concentration, verifying the origin of H_2 generated in the coupled reaction system. The oxidation reaction of BA is facilitated by the presence of H^+ ions [88], as photogenerated holes react with H^+ ions in water during the photocatalytic process, generating oxidizing agents that promote BA oxidation. Additionally, experimental evidence confirms that the H_2 protons in the coupled reaction system come from water molecules. This can be verified by isotopically labeling the water in the experimental system with D_2O. If the source of H_2 is indeed water molecules in the coupled reaction system, the production of D_2 would be observed when heavy water is used in the experiment. Therefore, through such experimental evidence, it can be confirmed that H_2 generated in the coupled photocatalytic H_2 evolution and BA oxidation reactions originates from water molecules. Therefore, in the CdS/U6N heterojunction, the synergistic effect of the different functionalities of CdS and U6N allows for the efficient utilization of photogenerated electrons and holes, enabling simultaneous H_2 production and the conversion of BA to BAD [89].

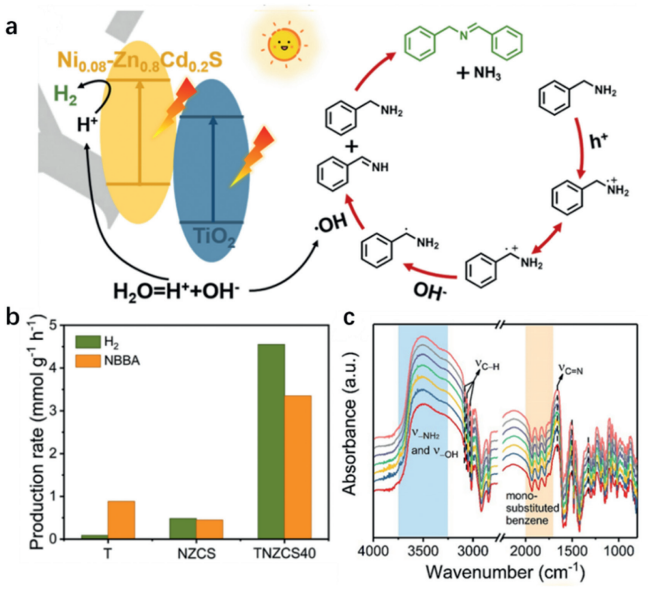

Fig. 5. (a) The proposed mechanism of photocatalytic benzylamine oxidation coupled with H_2 production over TNZCS40 surface. (b) The calculated H_2 and NBBA formation rates of H_2 (green) and NBBA (orange) over T, NZCS, and TNZCS40 in 12 h. (c) The *in situ* DRIFT spectra of TNZCS40 under illumination for 60 min after BA adsorption with the test interval of 10 min. Copied with permission [92]. Copyright 2023, Wiley-VCH.

4.3. Converting BA to NBBA coupling with H_2 production

The presence of imines, which contain a C=N bond [90], is crucial as an important intermediate for synthesizing quinoline derivatives, pyridine derivatives, and cucurbituril compounds. It holds significant significance in the fields of fine chemicals, pharmaceuticals, and agrochemical engineering. The selective oxidation of amines to imines combined with the generation of H_2 under anaerobic conditions is typically achieved by using precious metal catalysts such as palladium and platinum to enhance overall performance [91]. However, the high cost of these catalysts poses a challenge for industrial production. Therefore, the design of cost-effective and highly active photocatalysts is imperative. Emphasizing the role of imines in this passage, their importance lies in being a vital intermediate for synthesizing various compounds in the mentioned fields.

He *et al.* designed a $TiO_2/Ni_{0.08}$-$Zn_{0.2}Cd_{0.8}S$ quantum dot material by introducing nickel doping and constructing an S-scheme heterostructure [92]. This material was employed to enhance H_2 production and the oxidation reaction of benzylamine (BA). The research provides a method for further controlling the active sites and internal electric fields of S-scheme heterostructures. Additionally, the study serves as a reference for investigating other photocatalytic redox reactions.

In an S-scheme heterojunction, H_2 generation occurs on highly active sites featuring Ni^{2+}, while the oxidation of benzylamine takes place on the Lewis acidic [93] sites of the TiO_2 surface (Fig. 5a). Regarding the evolution process of NBBA, benzylamine is initially transformed into a benzylamine radical cation through photo-induced hole conversion. Subsequently, the benzylamine radical cation promptly converts into a nitrogen-centered radical through proton transfer reaction with OH^-. This process simultaneously generates H_2O molecules. Then, the newly formed radical undergoes intramolecular H_2 migration, resulting in the conversion into a more stable carbon-centered radical. Following this, the hole oxidizes OH^- to form a hydroxyl group, while the carbon-centered radical reacts with H_2O molecule hole oxidizes OH^- s to produce an imine intermediate (Ph-CH=NH) [94]. Ultimately, the Ph-CH=NH intermediate undergoes condensation reaction with benzylamine, leading to the release of NH_3 molecules and the formation of benzylidenebenzylamine (NBBA). Within a 12-h period, TNZCS 40 demonstrated the highest NBBA production rate of 3.35 mmol g^{-1} h^{-1} and an H_2 production rate of 4.55 mmol g^{-1} h^{-1}. In contrast, the original T and NZCS exhibited lower NBBA yields of 0.88 and 0.45 mmol g^{-1} h^{-1}, respectively, owing to inadequate redox capacity and pronounced charge recombination (Fig. 5b). In the experiment, BA vapor was initially introduced and under dark conditions, BA molecules adsorbed onto the Lewis acidic sites on the surface [95]. The broad peak observed in Fig. 5c (in the range of 3750–3250 cm^{-1}) can be attributed to the stretching vibrations of amino (N–H) and hydroxyl (O–H) groups in BA and H_2O, respectively. Additionally, peaks observed at 3082, 3060, and 3033 cm^{-1} correspond to the stretching vibrations of the methylene ($-CH_2$) groups attached to the benzene ring [96]. Moreover, the peak at 1460 cm^{-1} represents the asymmetric bending vibration of the C-H bonds in the benzene ring's side. The characteristic vibrational band for mono-substituted benzene is located between 1700–2000 cm^{-1}. Another twisting vibration peak of the benzene ring is also observed at 1502 cm^{-1}.

4.4. Converting OPD to 2MBZ coupling with H_2 production

Benzimidazole [97] compounds are widely used in the pharmaceutical and agrochemical fields for purposes such as treating infections and protecting crops. In recent years, extensive research has been conducted on the synthesis of benzimidazoles [98]. The common synthesis method involves the coupling reaction of *o*-phenylenediamine (OPD) with carboxylic acids or their derivatives under acidic and high-temperature conditions. However, this method often leads to the formation of many byproducts. Alternatively, benzimidazoles can be synthesized through the condensation reaction of OPD with aldehydes, but this method requires the use of stoichiometric or excess reagents and unwanted strong oxidants [99]. Faced with these challenges, there is an urgent need to develop an economically and environmentally friendly alternative method for the synthesis of benzimidazoles under mild reaction

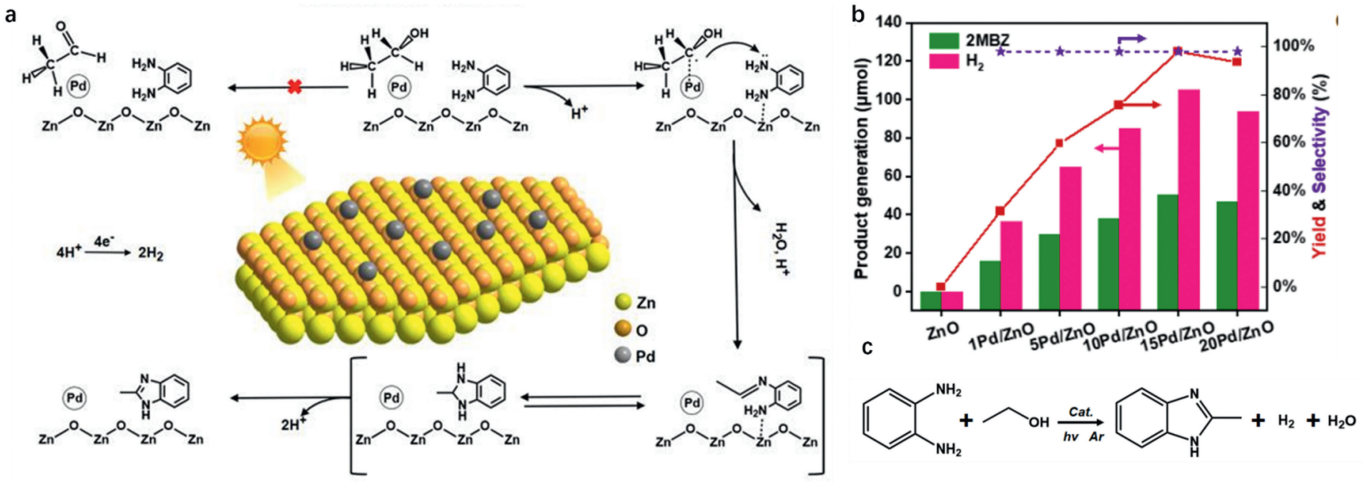

Fig. 6. (a) Proposed reaction mechanism for photocatalytic 2MBZ synthesis and H_2 evolution over 15Pd/ZnO. (b) Photocatalytic performance over pristine ZnO and Pd/ZnO composites with different contents of Pd after 4 h of illumination. (c) Formula for the cross-coupling of OPD and ethanol. Copied with permission [98]. Copyright 2023, Wiley-VCH.

conditions to address issues associated with traditional methods, including harsh reaction conditions, high energy consumption, and poor product selectivity.

Currently, the synthesis of benzimidazoles from alcohols and OPD involves the oxidation and deration of alcohols to generate aldehyde intermediates, which are then condensed with OPD to form benzimidazoles. However, the traditional synthesis route has a potential drawback, as the accumulation of aldehyde intermediates may lead to the generation of undesired byproducts, thereby reducing the selectivity of the desired benzimidazoles. In this context, the development of a new synthesis route to achieve more effective benzimidazole synthesis remains an ideal objective [100]. Particularly, the latest research direction in photocatalysis provides us with new perspectives and possible solutions. By utilizing photocatalytic technology, we can achieve the synthesis of benzimidazoles under milder conditions, thereby reducing energy consumption and improving product selectivity, offering new possibilities for addressing the issues present in traditional synthesis routes [101]. This integration of the latest research findings in photocatalysis not only fills existing research gaps but also holds the potential to provide new insights and methodologies for achieving more effective benzimidazole synthesis, with significant theoretical and practical implications.

Benzimidazole compounds have wide-ranging applications in the pharmaceutical and materials fields, making it of great importance to develop efficient synthetic methods for their research and practical applications. Wang *et al.* has developed a novel synthetic approach utilizing Pd-modified ultrathin ZnO nanocrystals as catalysts [102]. This approach promotes a mild and efficient cross-coupling reaction between alcohols and OPD, enabling the synthesis of benzimidazole compounds while concurrently producing H_2. This method demonstrates high efficiency and environmental friendliness, thus opening up a new avenue for the synthesis of benzimidazole compounds.

Rational photocatalytic reaction mechanism of benzimidazole synthesis with concurrent H_2 generation (Fig. 6a). Under light illumination, the 15Pd/ZnO catalyst generates photoinduced charge carriers. The interface interaction between Pd NPs and ZnO NS promotes efficient separation and transfer of the photoinduced charge carriers. In contrast to previous reports involving the conversion of ethanol to acetaldehyde followed by condensation with diamines, the presence of Pd NPs facilitates the selective cleavage of the α-C−H bond of ethanol, generating highly reactive $^{\bullet}CH(CH_3)$ OH species and providing strong adsorption sites. Moreover, the exposed unsaturated metal centers on the 15Pd/ZnO catalyst surface act as Lewis acid sites, favoring the adsorption of OPD [103]. Subsequently, the highly active $^{\bullet}CH(CH_3)$ OH attacks the lone pair electrons of the $-NH_2$ group on OPD, forming a Schiff base. Finally, the Schiff base undergoes further deration and cyclization reactions to yield 2-methylbenzimidazole (2MBZ). Simultaneously, the photo-generated holes interact with protons and reduce them to H_2. Based on the above findings, we propose a rational photocatalytic reaction mechanism for the synthesis of benzimidazole accompanied by H_2 generation. The catalytic activity of Pd/ZnO composite material is significantly enhanced. Initially, no gas or liquid products were detected on the pristine ZnO catalyst. However, the catalytic activity significantly improved when Pd nanoparticles were deposited on ZnO to form the composite material. In particular, the 15% Pd/ZnO composite exhibited the best catalytic performance, with a production rate of 1.2 mmol g^{-1} h^{-1} of 2MBZ and 2.5 mmol g^{-1} h^{-1} of H_2, while maintaining a remarkable selectivity of 98%. Additionally, the observed changes in the yield of 2MBZ in the prepared samples shown in Fig. 6b indicate a strong correlation between the formation of 2MBZ and the Pd modification, further confirming the crucial role of Pd in this reaction process [104]. Based on the stoichiometric ratio of 2MBZ to H_2, it can be inferred that the consumption ratio of electrons and holes in the redox reaction is approximately 2:1, suggesting a stoichiometric deration reaction. The *in-situ* Fourier-transform infrared (FT-IR) technique was utilized to further investigate the synthesis pathway of 2MBZ. Prior to the *in-situ* FT-IR measurements, the 15Pd/ZnO catalyst was subjected to OPD ethanol solution adsorption treatment in Ar atmosphere for 30 min. Through a photooxidation-reduction-driven reaction (Fig. 6c), the simultaneous synthesis of 2MBZ and generation of H_2 is achieved in an Ar atmosphere by utilizing OPD and ethanol as starting materials.

4.5. Converting FOL to FAL and coupling with H_2 production

Recently, some studies have utilized photocatalysis as a new method to promote the synthesis of furfural and the generation of H_2 [105]. By designing and synthesizing materials with excellent photocatalytic activity, these studies are dedicated to converting visible light into the energy required for chemical reactions, thereby enhancing reaction efficiency and reducing energy consumption. In addition, photocatalysis can selectively promote the production of furfural, reducing the generation of by-products. Compared to traditional thermal chemical methods, photocataly-

sis can provide milder and more environmentally friendly reaction conditions, and has the potential to achieve efficient energy utilization and the realization of green chemical processes [106]. However, despite the many potential advantages of research on promoting furfural synthesis and H_2 generation through photocatalysis, there are still some challenges. These challenges include the synthesis and optimization of photocatalysts, control of reaction conditions, catalyst stability, and recycling [107], among others. Furthermore, the efficiency and yield of promoting furfural synthesis through photocatalysis still need to be further improved to meet the needs of industrial applications. In conclusion, promoting furfural synthesis and H_2 generation through photocatalysis is a research direction with significant potential. Through photocatalysis, we have the potential to achieve efficient, environmentally friendly, and sustainable furfural synthesis, providing new possibilities for green chemistry and renewable energy production.

Recent research developments have indicated that using visible light catalysis for the water splitting reaction can effectively generate H_2. In this regard, Yang *et al.* have successfully synthesized a sample with outstanding photocatalytic activity [108]. To explore its photocatalytic activity, they utilized FOL (an aqueous alcohol solution, furfuryl alcohol) as a hole sacrificial reagent to further enhance the efficiency of the water splitting reaction. They exposed the prepared sample to visible light irradiation and introduced FOL into the reaction system [109]. The photocatalyst absorbs visible light energy, exciting electrons and holes, thereby creating active sites on the material surface. FOL acts as a hole sacrificial reagent, capturing and eliminating the generated holes, thus sustaining the photocatalytic reaction [110]. Under these reaction conditions, water molecules were effectively decomposed into H_2 and O_2. Through the rational design and optimization of the photocatalyst's characteristics of the photocatalysts, Yang *et al.* achieved efficient photocatalytic H_2 generation. Additionally, this study successfully integrated the utilization of FOL with the production of valuable furfuraldehyde (FAL), thereby achieving effective resource utilization and value enhancement [111]. This photocatalyst-based water splitting reaction not only provides an environmentally friendly and sustainable method for H_2 production, but also contributes to the simultaneous production of valuable FAL, thereby realizing the goal of green chemistry. This research demonstrates the practical application of the latest research developments in the field of photocatalysis, providing important insights for the production and efficient utilization of renewable energy.

Under visible light, as shown in Fig. 7a, the ZIS shell gets energized and sends its electrons to the MC core, thanks to the unique way these particles are put together. These electrons are crucial in breaking down water into H_2, while the remaining energy in the shell takes a molecule called FOL and turns it into FAL, a more valuable chemical. The clever design of MC@ZIS ensures that the energy from the light is used effectively, increasing the production of both H_2 and FAL. As observed in Fig. 7b, the pristine ZIS exhibits a relatively low H_2 production rate of only 0.116 mmol g^{-1} h^{-1}, with MC showing little activity towards the photo-oxidation-reduction reaction. However, with the fabrication of the core-shell Schottky junction between ZIS and MC, there is a substantial increase in the rate of H_2 generation. Notably, the H_2 production rate for 1.5%MC@ZIS reaches 2.80 mmol g^{-1} h^{-1}, which is 24.1 times higher than that of the pristine ZIS and nearly 1.9 times higher than that of 1.5%Pt-ZIS. This underscores the critical role of MC as an effective non-precious metal cocatalyst in photocatalytic HER [112].

The findings confirm the potential of MC in enhancing catalytic performance, paving the way for the development of cost-effective and efficient photocatalytic systems for H_2 production. Most im-

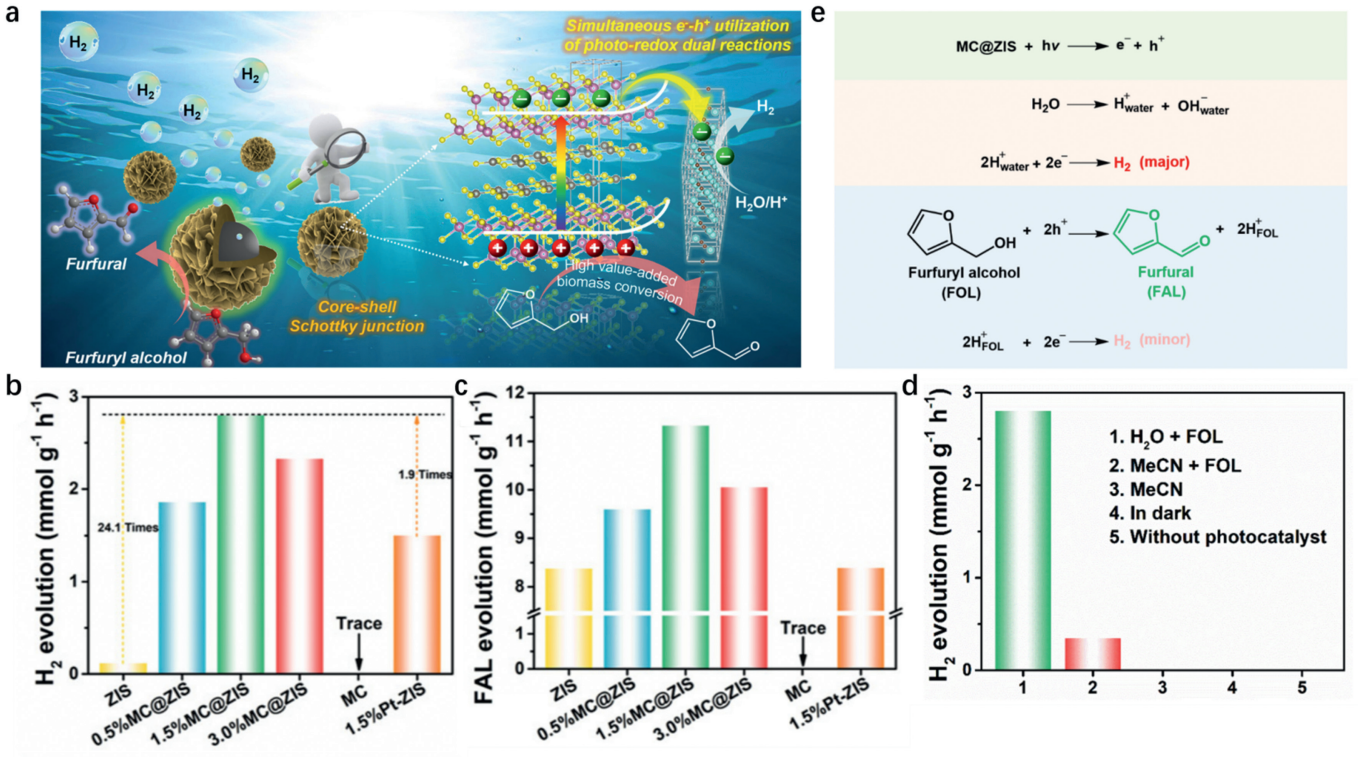

Fig. 7. (a) Proposed photocatalytic reaction mechanism of cooperative photo-redox dual reactions for H_2 evolution and valuable FAL production over the core–shell MC@ZIS Schottky junction under visible light irradiation. (b) The corresponding H_2 yield rates over the as-prepared samples in the aqueous solution of FOL. (c) The corresponding H_2 yield rates over the as-prepared samples in the aqueous solution of FOL. (d) Photocatalytic H_2 production rates of the prepared 1.5%MC@ZIS Schottky junction under different reaction conditions. (e) The formulas of photo-redox dual reactions for integrating H_2 evolution and the FAL production. Copied with permission [108]. Copyright 2023, Royal Society of Chemistry.

Table 1
Recent key works on coupling organic synthesis and H_2 production.

Precursor	Products	H_2 production rate	Organics production rate	Ref.
Biomass	Formic acid	14386 μmol g^{-1} h^{-1}	372 μmol g^{-1} h^{-1}	[75,78]
Benzyl alcohol	Benzaldehyde	38.1 μmol g^{-1} h^{-1}	37.8 μmol g^{-1} h^{-1}	[84]
Benzylamine	*N*-Benzylidenebenzylamine	4.55 mmol g^{-1} h^{-1}	3.35 mmol g^{-1} h^{-1}	[92]
OPD	2MBZ	1.2 mmol g^{-1} h^{-1}	2.5 mmol g^{-1} h^{-1}	[98]
Furfuryl alcohol	Furfural	11.33 mmol g^{-1} h^{-1}	2.80 mmol g^{-1} h^{-1}	[108]

portantly, as demonstrated in Fig. 7c, the integration of the cocatalyst MC contributes to an impressive enhancement in the photocatalytic production rate of FAL. The FAL yield for 1.5%MC@ZIS (11.33 mmol g^{-1} h^{-1}) is significantly higher than that observed for pristine ZIS (8.38 mmol g^{-1} h^{-1}) and 1.5%Pt-ZIS (8.39 mmol g^{-1} h^{-1}). It is noteworthy that there appears to be a coarse correlation between the MC content and the H_2/FAL production. The specialized ability of the MC@ZIS Schottky junction to yield both H_2 and FAL can be attributed to its unique core-shell architecture, which promotes enhanced photogenerated carrier transfer. However, the excessive introduction of MC does not favor the evolution of H_2 or the conversion of FOL, which is likely due to the photoblocking effect [113]. Simultaneously, an overabundance of MC could hinder the photocatalytic active sites of ZIS, thereby adversely affecting its photo-oxidation-reduction performance. This balance indicates the necessity for optimization of MC content to maximize photocatalytic activity while avoiding detrimental effects on the transformation processes.

Subsequent controlled experiments were conducted to explore the effects of experimental conditions on the photocatalytic performance of the 1.5%MC@ZIS core-shell Schottky junction. As depicted in Fig. 7d, no H_2 production was detected in the absence of the photocatalyst or upon cessation of visible light irradiation, unequivocally indicating that the reaction is photocatalytically driven. When acetonitrile (MeCN) was used as a solvent in place of H_2O, the H_2 production rate for 1.5%MC@ZIS dramatically decreased to 0.34 mmol g^{-1} h^{-1}, and no H_2 generation occurred in pure MeCN solvent [114]. These results confirm that the protons reduced by photogenerated electrons to form H_2 predominantly originate from the disassociation of H_2O, rather than the deration of FOL. Therefore, the produced H_2 is mainly sourced from the splitting of water, with a minor contribution from the deration of FOL (Fig. 7e). In this photo-oxidation-reduction reaction system, FOL can not only replace traditional, costly hole scavengers (such as triethanolamine, Na_2S/Na_2SO_3) but also generate valuable chemical products during the H_2 production process. This holds great significance for the green and sustainable valorization of photo-induced holes [115], enhancing the overall appeal and practicality of photocatalytic systems for H_2 generation. Table 1 summarizes the significant work in recent years on coupling organic synthesis and H_2 production.

5. Summary and outlook

In summary, to realize the industrialization and sustainable development of photocatalytic H_2 production technology, concerted efforts in the investigation of catalytic mechanisms, innovation in characterization techniques, optimization of reaction conditions, and large-scale implementation are necessary. Through such endeavors, we aim to continuously enhance the efficiency of photocatalytic H_2 production, advancing its application in the field of energy conversion and storage, ultimately ensuring the reliable supply and clean utilization of renewable energy resources. As shown in Fig. 8, the photocatalytic coupling strategy for H_2 production summarizes the key points of the entire article.

In the field of photocatalytic H_2 production research, there exists vast room for continual advancement and refinement.

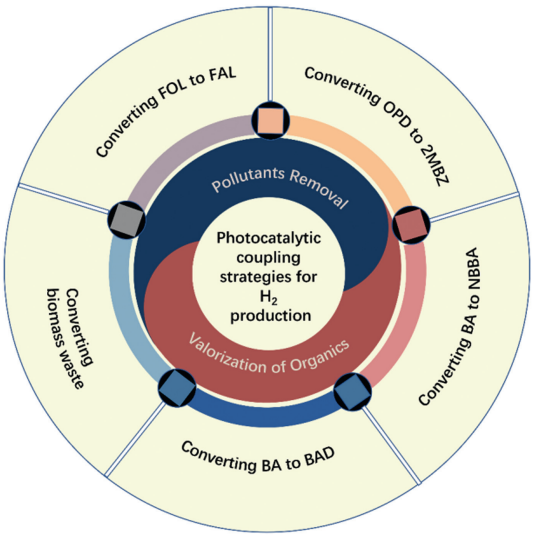

Fig. 8. Photocatalytic coupling strategies for H_2 production.

(1) In the array of strategies for photocatalytic H_2 production, standardized testing for the evaluation of catalytic H_2 production performance is essential and warrants heightened attention to ensure comparability and accuracy of results. A pivotal direction for future research lies in delving into the complex coupling relationship between the provenance of protons, the reduction reactions producing H_2, and the oxidation reactions. Moreover, isotope labeling techniques, particularly proton-deuteron exchange, are crucial in probing the mechanisms of catalytic reactions, facilitating the revelation of reaction pathways and the formation processes of intermediate products, thus enabling a more precise understanding and optimization of the catalytic process.
(2) There is a clear mandate to enhance current research methodologies, especially through innovative advancements in characterization techniques. Employing visual technologies to augment the observation of oxidation and reduction reactions at various catalytic interfaces opens the possibility of gaining novel insights into the kinetics of catalytic reactions. Real-time visual analysis will assist in elucidating the microscopic origins of catalytic activity and the interfacial interactions occurring throughout the reaction process.
(3) Future research should strive to further harmonize oxidation and reduction reactions, ensuring not only compatibility of reaction rates but also considering the strategic inclusion of catalysts to facilitate specific oxidation reactions. In this way, we can refine the overall reaction rates and utilize light energy more efficiently for H_2 production.
(4) As current studies are still in the nascent stage, the construction of large-scale photocatalytic H_2 production apparatuses is imperative to move towards practical application and demonstrate its industrial value. The establishment of large-scale facilities will contribute to assessing the scalabil-

ity, stability, and economic viability of the technology, serving as a vital step in transitioning from laboratory research to commercial application.

Declaration of competing interest

The authors declare that they have no known competing financial interests or personal relationships that could have appeared to influence the work reported in this paper.

CRediT authorship contribution statement

Yuehai Zhi: Writing – review & editing, Writing – original draft, Formal analysis. **Chen Gu:** Writing – original draft, Investigation. **Huachao Ji:** Software, Investigation. **Kang Chen:** Investigation, Formal analysis. **Wenqi Gao:** Software, Methodology, Investigation. **Jianmei Chen:** Writing – review & editing. **Dafeng Yan:** Writing – review & editing, Writing – original draft, Supervision, Funding acquisition.

Acknowledgment

This work was financially supported by the National Natural Science Foundation of China (No. 22202065).

References

[1] J.L. Holechek, H.M. Geli, M.N. Sawalhah, R. Valdez, Sustainability 14 (2022) 4792.
[2] P. Carter, BMJ-Brit. Med. J. 374 (2021) 2369.
[3] E. David, V. Stanciu, C. Sandru, et al., WIT Press 102 (2007) 923–932.
[4] G.D. Thurston, Environ. Int. 160 (2022) 107066.
[5] A. Raza, Y. Zhang, A. Cassinese, et al., Catalysts 12 (2022) 1613.
[6] A. Jain, D. Vaya, J. Chil. Chem. Soc. 62 (2017) 3683–3690.
[7] L. Noureen, Q. Wang, M. Humayun, et al., Environ. Res. 219 (2023) 115084.
[8] V.M. Daskalaki, M. Antoniadou, G.L. Puma, et al., Environ. Sci. Techno. 44 (2010) 7200–7205.
[9] M. Ikram, A. Raza, S.O.A. Ahmad, et al., Adv. Mater. Interfaces 10 (2023) 2202172.
[10] S. Kumar, A. Kumar, A. Bahuguna, et al., Beilstein J. Nanotech. 8 (2017) 1571–1600.
[11] S. Crawford, E. Thimsen, P. Biswas, J. Electrochem. 156 (2009) H346–H351.
[12] T. Hisatomi, J. Kubota, K. Domen, Chem. Soc. Rev. 43 (2014) 7520–7535.
[13] W. Huang, C. Su, C. Zhu, et al., Angew. Chem. 135 (2023) e202304634.
[14] J. Yang, D. Wang, H. Han, et al., Acc. Chem. Res. 46 (2013) 1900–1909.
[15] M. Pirila, M. Saouabe, S. Ojala, et al., Top. Catal. 58 (2015) 1085–1099.
[16] E.M. Akinoglu, D.A. Hoogeveen, C. Cao, et al., ACS Nano 15 (2021) 7860–7878.
[17] S. Nayak, G. Swain, K. Parida, ACS Appl, Mater. Inter. 11 (2019) 20923–20942.
[18] F. Sun, Y. Xie, D. Xu, et al., J. Environ. Chem. Eng. 11 (2023) 109169.
[19] H. Zhang, Y. Wan, S. Shang, et al., Dalton Trans. 52 (2023) 4562–4573.
[20] S. Lettieri, M. Pavone, A. Fioravanti, et al., Materials 14 (2021) 1645.
[21] K. Perovic, F.M. dela Rosa, M. Kovacic, et al., Materials 13 (2020) 1338.
[22] K. Poonia, P. Singh, A. Singh, et al., Environ. Chem. Lett. 21 (2023) 265–283.
[23] Q. Lin, Y.H. Li, M.Y. Qi, et al., Appl. Catal. B: Environ. 271 (2020) 118946.
[24] B. You, G. Han, Y. Sun, Chem. Commun. 54 (2018) 5943–5955.
[25] Y. Li, F. Zhang, Y. Chen, et al., Green Chem. 22 (2020) 163–169.
[26] T. Matamba, A. Tahmasebi, J. Yu, et al., J. Anal. Appl. Pyrol. 175 (2023) 106221.
[27] Z. Cheng, Y. He, C. Yang, et al., Chin. Chem. Lett. 34 (2023) 1001–8417.
[28] K. Hashimoto, T. Kawai, T. Sakata, J. Phys. Chem. C 88 (1984) 4083–4088.
[29] F. Zeng, C. Mebrahtu, L. Liao, et al., J. Energy Chem. 69 (2022) 301–329.
[30] K. Ahmad, H.R. Ghatak, Environ. Technol. 19 (2020) 100893.
[31] N.M. Gupta, Renew. Sust. Energ. Rev. 71 (2017) 585–601.
[32] A.A. Mutalib, N. Jaafar, Environ. Chem. Lett. 3 (2022) 100013.
[33] T. Ochiai, A. Fujishima, J. Photoch. Photobio. C 13 (2012) 247–262.
[34] J.O.M. Bockris, T.N. Veziroglu, Environ. Conserv. 12 (1985) 105–118.
[35] P. Gómez-López, A. Puente-Santiago, A. Castro-Beltrán, et al., Curr. Opin. Green Sust. 24 (2020) 48–55.
[36] Y. Xu, M.A. Schoonen, Am. Mineral 85 (2000) 543–556.
[37] Q. Huang, X. Liu, Z. Zhang, et al., Chin. Chem. Lett. 34 (2023) 108046.
[38] G.S. Shanker, A. Biswas, S. Ogale, J. Phys. Energy 3 (2021) 022003.
[39] S. Yu, Y. Li, A. Jiang, et al., Adv. Energy Mater. 14 (2024) 2304362.
[40] S.O. Amrouche, D. Rekioua, T. Rekioua, et al., Int. J. Hydrogen Energ. 41 (2016) 20914–20927.
[41] L. Roza, V. Fauzia, M.Y. Abd Rahman, Surf. Interfaces 15 (2019) 117–124.
[42] A.K. Ganguli, G.B. Kunde, W. Raza, et al., Molecules 27 (2022) 7778.
[43] D.S. Constantino, M.M. Dias, A.M. Silva, et al., J. Clean Prod. 340 (2022) 130800.
[44] X.H. Jiang, L.C. Wang, F. Yu, et al., ACS Sustain. Chem. Eng. 6 (2018) 12695–12705.
[45] R. Duarte-Davidson, C. Courage, L. Rushton, L. Levy, Occup. Environ. Med. 58 (2001) 2–13.
[46] A. Smith, Occup. Med-Oxford 42 (1992) 83–88.
[47] F. Fu, Q. Wang, J. Environ. Manage 92 (2011) 407–418.
[48] M. Qi, Y. Xu, Angew. Chem. 135 (2023) e202311731.
[49] C. Han, Y. Li, J. Li, et al., Angew. Chem. Int. Ed. 60 (2021) 7962–7970.
[50] F. Wang, H. Ji, Z. Wu, et al., Chin. Chem. Lett. (2024), doi:10.1016/j.cclet.2024.109898.
[51] J. Li, Y. Feng, F. Fu, X. Xin, et al., Chin. Chem. Lett. 35 (2024) 108736.
[52] N. Mchedlov-Petrosyan, Y.V. Kholin, Russ. J. Appl. Chem. 77 (2004) 414–422.
[53] M. Majek, F. Filace, A.J. von Wangelin, Beilstein J. Org. Chem. 10 (2014) 981–989.
[54] S. Haydar, M. Ferro-Garcıa, J. Rivera-Utrilla, et al., Carbon 41 (2003) 387–395.
[55] H. Tian, C. Wan, X. Xue, et al., Catalysts 7 (2017) 156.
[56] Z. Wei, J. Liu, W. Shangguan, Chin. J. Catal. 41 (2020) 1440–1450.
[57] J. Deng, Y.X. Zeng, E. Almatrafi, et al., Coord. Chem. Rev. 505 (2024) 215693.
[58] Y. Bai, C. Liu, Y. Shan, et al., Adv. Energy Mater. 12 (2022) 2100346.
[59] D.T. Tran, T.H. Nguyen, H. Jeong, et al., Nano Energy 94 (2022) 106929.
[60] N. Yang, Y. Tian, M. Zhang, et al., Biotechnol. Adv. 54 (2022) 107808.
[61] X. Shao, Y. Wang, M. Qi, et al., Mol. Catal. 557 (2024) 113991.
[62] X.C. Dai, M.H. Huang, Y.B. Li, et al., J. Mater. Chem. A 7 (2019) 2741–2753.
[63] G. Zhou, Z. Zhou, Y. Xia, et al., Appl. Surf. Sci. 608 (2023) 154974.
[64] K. Ahmad, H.R. Ghatak, S. Ahuja, Environ. Technol. Inno. 19 (2020) 100893.
[65] F. Wang, Q. Li, D. Xu, Adv. Energy Mater. 7 (2017) 1700529.
[66] W. Tang, L. Zhang, T. Qiu, et al., Angew. Chem. 135 (2023) e202305843.
[67] D. Zhang, P. Wang, F. Chen, et al., Chin. Chem. Lett. 31 (2020) 2795–2798.
[68] D. Chen, Y. Cheng, N. Zhou, et al., J. Clean Prod. 268 (2020) 121725.
[69] E.J. Cho, L.T.P. Trinh, Y. Song, et al., Bioresource Technol. 298 (2020) 122386.
[70] G. Liao, C. Li, S.Y. Liu, et al., Phys. Rep. 983 (2022) 1–41.
[71] R. Ahmad, Z. Ahmad, A.U. Khan, et al., J. Environ. Chem. Eng. 4 (2016) 4143–4164.
[72] A. Rani, Y. Zhao, Q. Yan, et al., Anal. Chem. 95 (2023) 4871–4879.
[73] M.L. Sundar, K.M. Nampoothiri, Bioresource Technol. 345 (2022) 126548.
[74] W. Li, X. Zhen, B.B. Xu, et al., Angew. Chem. Int. Ed. 63 (2024) e202320014.
[75] T. Wang, L. Tao, X. Zhu, et al., Nat. Catal. 5 (2022) 66–73.
[76] Z. Jiang, Y. Zeng, D. Hu, et al., Green Chem. 25 (2023) 871–892.
[77] M.Y. Qi, M. Conte, M. Anpo, et al., Chem. Rev. 121 (2021) 13051–13085.
[78] B. Liu, J. Cai, J. Zhang, et al., Chin. J. Catal. 51 (2023) 204–215.
[79] J. Luo, M. Wang, L. Chen, et al., J. Energy Chem. 66 (2022) 52–60.
[80] M.Y. Qi, Y.H. Li, M. Anpo, et al., ACS Catal. 10 (2020) 14327–14335.
[81] W. Zhang, J. Hou, M. Bai, et al., Chin. Chem. Lett. 34 (2023) 108270.
[82] W. Liu, P. Fu, Y. Zhang, et al., Chem. Rev. 121 (2021) 13051–13085.
[83] J. Liu, J. Wan, L. Liu, et al., Chem. Eng. J. 430 (2022) 133125.
[84] Y.X. Zeng, J. Deng, N. Zhou, et al., Small 20 (2024) 2311552.
[85] H.J. Liang, P. Hua, Y. Zhou, et al., Chin. Chem. Lett. 30 (2019) 2245–2248.
[86] B. He, P. Xiao, S. Wan, et al., Angew. Chem. Int. Ed. 62 (2023) e202313172.
[87] G. Sirvinskaite, J.C. Reisenbauer, B. Morandi, Chem. Sci. 14 (2023) 1709–1714.
[88] S. Wu, Y.F. Zhang, H. Ding, et al., J. Colloid Interf. Sci. 610 (2022) 446–454.
[89] C. Bo, L. Lei, Z.j. Diao, et al., J. Fuel Chem. Technol. 50 (2022) 621–627.
[90] B. Pathare, T. Bansode, Results Chem. 3 (2021) 100200.
[91] Y.F. Wang, M.Y. Qi, M. Conte, et al., Angew. Chem. 135 (2023) e202304306.
[92] M.A. Tzani, C. Gabriel, I.N. Lykakis, Nanomaterials 10 (2020) 2405.
[93] T. Montini, V. Gombac, J.J. Delgado, et al., Inorg. Chim. Acta 520 (2021) 120289.
[94] D. Chanda, G.M. Venkataswamy, L.V. Hipparagi, et al., Synthetic Commun. 51 (2021) 3379–3389.
[95] S. Dhingra, M. Sharma, V. Krishnan, et al., J. Colloid Interf. Sci. 608 (2022) 1040–1050.
[96] R. Zhu, G. Zhou, J.n. Teng, et al., Green Chem. 23 (2021) 1758–1765.
[97] S.C. Kosloski-Oh, Z.A. Wood, Y. Manjarrez, et al., Mater. Horiz. 8 (2021) 1084–1129.
[98] F.K. Shang, Y.H. Li, M.Y. Qi, et al., Catalysis Today 410 (2023) 85–101.
[99] J. Wang, X. Liu, Z. Li, Chem. Asian J. 16 (2021) 2932–2938.
[100] R. Ghalta, R. Srivastava, Sustain. Energ. Fuels 7 (2023) 1707–1723.
[101] Y. Yuan, J. Pan, W.N. Yin, et al., Chin. Chem. Lett. 35 (2024) 108724.
[102] C.I. Ezugwu, S. Ghosh, S. Bera, et al., Sep. Purif. Technol. 308 (2023) 122868.
[103] W. Zou, H. Zhou, M. Wang, ChemSusChem 16 (2023) e202300727.
[104] W. Liu, P. Fu, Y. Zhang, et al., Proc. Natl. Acad. Sci. U. S. A. 120 (2023) e2218813120.
[105] B. Xia, Y. Zhang, B. Shi, et al., Small Methods 4 (2020) 2000063.
[106] Y. Chen, M. Qi, Z. Tang, Mol. Catal. 561 (2024) 114178.
[107] F. Xing, R. Zeng, C. Cheng, et al., Appl. Catal. B: Environ. 306 (2022) 121087.
[108] L. Gao, W. Xiao, M. Qi, et al., Mol. Catal. 554 (2024) 113858.
[109] J. Yang, X. Zhang, Z. Zeng, et al., Inorg. Chem. Front. 10 (2023) 6308–6319.
[110] X. Sun, M. Song, F. Liu, et al., Appl. Catal. B: Environ. 342 (2024) 123436.
[111] M. Qi, Marco Conte, Z Tang, et al., ACS Nano 16 (2022) 17444–17453.
[112] X. Liu, S. Zhang, M. Wang, et al., Chin. Chem. Lett. 35 (2024) 108723.
[113] Q. Xiang, J. Yu, P.K. Wong, J. Colloid Interf. Sci. 357 (2011) 163–167.
[114] L. Yuan, M. Qi, Z Tang, et al., Angew. Chem. Int. Ed. 60 (2021) 21150–21172.
[115] D. Yan, C. Mebrahtu, S. Wang, et al., Angew. Chem. Int. Ed. 62 (2023) e202214333.